Liposomal Quercetin Efficiently Suppresses Growth of Solid Tumors in Murine Models

Zhi-ping Yuan, Li-juan Chen, Lin-yu Fan, Ming-hai Tang, Guang-li Yang, Han-su Yang, Xiao-bo Du, Guo-qing Wang, Wen-xiu Yao, Qu-mei Zhao, Bin Ye, Rui Wang, Peng Diao, Wei Zhang, Hong-bin Wu, Xia Zhao, and Yu-Quan Wei

Abstract

Purpose: Quercetin is a potent chemotherapeutic drug. Clinical trials exploring different schedules of administration of quercetin have been hampered by its extreme water insolubility. To overcome this limitation, this study is aimed to develop liposomal quercetin and investigate its distribution *in vivo* and antitumor efficacy *in vivo* and *in vitro*.

Experimental Design: Quercetin was encapsulated in polyethylene glycol 4000 liposomes. Biodistribution of liposomal quercetin i.v. at 50 mg/kg in tumor-bearing mice was detected by high-performance liquid chromatography. Induction of apoptosis by liposomal quercetin *in vitro* was tested. The antitumor activity of liposomal quercetin was evaluated in the immunocompetent C57BL/6N mice bearing LL/2 Lewis lung cancer and in BALB/c mice bearing CT26 colon adenocarcinoma and H22 hepatoma. Tumor volume and survival time were observed. The mechanisms underlying the antitumor effect of quercetin *in vivo* was investigated by detecting the microvessel density, apoptosis, and heat shock protein 70 expression in tumor tissues.

Results: Liposomal quercetin could be dissolved in i.v. injection and effectively accumulate in tumor tissues. The half-time of liposomal quercetin was 2 hours in plasma. The liposomal quercetin induced apoptosis *in vitro* and significantly inhibited tumor growth *in vivo* in a dose-dependent manner. The optimal dose of liposomal quercetin resulted in a 40-day survival rate of 40%. Quantitative real-time PCR showed that liposomal quercetin down-regulated the expression of heat shock protein 70 in tumor tissues. Immunohistochemistry analysis showed that liposomal quercetin inhibited tumor angiogenesis as assessed by CD31 and induced tumor cell apoptosis.

Conclusions: Our data indicated that pegylated liposomal quercetin can significantly improve the solubility and bioavailability of quercetin and can be a potential application in the treatment of tumor.

Quercetin (3,3′,4′,5,7-pentahydroxyflavone) is a naturally occurring flavone found in the plant kingdom. It is a component of most edible fruits and vegetables, with the highest concentrations being found in onions, apples, and red wine (1, 2). Quercetin has many biological activities, such as antitumor and antiproliferative effects on a wide range of human cancer cell lines and inhibition of glycolysis, macromolecule synthesis, and enzymes (3–7). Its inhibition of the heat shock protein 70 (HSP70) synthesis and expression in tumor cells was reported in our previous work (8). Clinical trials exploring different schedules of administration of quercetin have been hampered by its extreme water insolubility requiring dissolution in DMSO. There are concerns about using higher doses of DMSO, as it causes dose-dependent hemolysis, it is harmful to the liver and kidneys, and it has an unpleasant odor for 48 hours after administration (9–11). A potential solution to this problem is to improve its solubility by chemical modification (12), but the decreased activity of quercetin was observed in our laboratory.

Liposomes have been used previously as carriers for delivery of a variety of drugs, including antibiotic, antifungal, and cytotoxic agents (13). As carriers for anticancer drugs, they have been shown to reduce side effect, such as anthracycline-induced cardiomyopathy (14). Liposomes accumulate preferentially at tumor sites because of their ability to extravasate through ''pores'' or ''defects'' in the capillary endothelium. These ''pores'' seem to be a consequence of the rapid angiogenesis occurring in tumors and are generally not present in normal tissues or organs (15). After coating the liposome surface with inert, biocompatible polymers, such as polyethylene glycol (PEG),

Authors' Affiliation: State Key Laboratory of Biotherapy, West China Hospital, West China Medical School, Sichuan University, Chengdu, Sichuan, People's Republic of China

Received 10/31/05; revised 3/8/06; accepted 3/16/06.

Grant support: National Basic Research Program of China grants 2001CB510001 and 2004CB518800, National Natural Science Foundation of China, and National 863 Program.

The costs of publication of this article were defrayed in part by the payment of page charges. This article must therefore be hereby marked *advertisement* in accordance with 18 U.S.C. Section 1734 solely to indicate this fact.

Requests for reprints: Yu-Quan Wei, State Key Laboratory of Biotherapy, West China Hospital, West China Medical School, Sichuan University, Chengdu, Sichuan 610041, People's Republic of China. Phone: 86-28-85164059; Fax: 86-28-85164063; E-mail: yuquawei@vip.sina.com or yuquawei@hotmail.com.

doi:10.1158/1078-0432.CCR-05-2365

it forms a protective layer over the liposome surface and slows down liposome recognition by opsonins and therefore subsequent clearance of liposomes, so that a liposome has a long circulation time and provides slow release of an encapsulated drug, resulting in sustained exposure to tumor cells and enhanced efficacy (16).

In the present work, we encapsulated quercetin in the nonaqueous interior of the PEG liposome. The pharmacokinetic properties and biodistribution in tumor-bearing mice were tested, and anticancer efficacy of liposomal quercetin was observed *in vivo* and *in vitro*.

Materials and Methods

Materials. High-purity lecithin of soybean, PEG 4000, glucosidase, cholesterol, and quercetin were purchased from Sigma Chemical Co. (St. Louis, MO). Cisplatin (DDP) was purchased from Qilu Pharmaceutical Co. (Shandong, China). A rat antimouse CD31 monoclonal antibody was purchased from BD Biosciences Co. (PharMingen, San Diego, CA). *In situ* Cell Death Detection kit was purchased from Roche Co. (Promega, Madison, WI) Real-time One-Step RNA PCR kit was purchased from TaKaRa Co. (Dalian, China).

Cell culture and tumor model. Mouse colorectal carcinoma cell line CT26, Lewis lung cancer cell line LL/2, and hepatoma cell line H22 were obtained from the American Type Culture Collection (ATCC, Manassas, VA). These cells were grown in RPMI 1640 (Life Technologies, Bedford, MA) or DMEM (Life Technologies) containing 10% heat-inactivated FCS, 100 units/mL penicillin, and 100 units/mL streptomycin in a humid chamber at 37°C under 5% CO_2.

The CT26 and H22 tumor models were established in 8-week-old female BALB/c mice. LL/2 tumor model was established in C57BL/6N mice as described previously (17). Briefly, these BALB/c mice were inoculated with CT26 or H22 cells (5×10^5) and C57BL/6N mice with LL/2 cells (1×10^6) s.c. in the dorsal area. All these mice were purchased from Sichuan University Animal Center (Sichuan, Chengdu, China). All studies involving mice were approved by the Institute's Animal Care and Use Committee.

Preparation of pegylated liposomal quercetin and empty pegylated liposomes. PEG-modified liposomal quercetin (Q-PEGL) were prepared in our laboratory and described briefly as follows: the mixtures of lecithin/cholesterol/PEG 4000/quercetin in 13:4:1:6 weight ratio were dissolved in chloroform/methanol (3:1, v/v) and evaporated to dryness under reduced pressure in a rotary evaporator. The dried lipid films were sonicated in 5% glucose solution at constant container followed by concentrated and lyophilized. The preparation of empty pegylated liposomes (PEGL) was the same way as the Q-PEGL without quercetin in the mixtures. The final Q-PEGL and the PEGL were small unilamellar liposomes in our studies and in a size range of 130 ± 20 and 100 ± 20 nm, respectively. In following studies, the dose of Q-PEGL was on a quercetin basis, and Q-PEGL or PEGL was dissolved in 5% glucose water.

Pharmacokinetic studies in tumor-bearing BABL/c mice. Female BABL/c mice ($n = 64$) were inoculated with CT26 cells. On day 15, the Q-PEGL or the free quercetin dissolved in DMSO was given i.v. to these mice at a dose of 50 mg/kg. Mice were sacrificed at defined time points (5, 15, 30, 60, 120, 240, 720, and 1,440 minutes). At each time point, four mice were sacrificed and their blood was collected from the orbital cavity vein plexus, heparinized, and centrifuged to obtain the plasma. The tumor, kidney, liver, lung, intestine, heart, and spleen tissues were excised and weighed, and homogenized. Glucosidase was added into plasma sample and incubated in 37°C for 2 hours. Plasma and the homogenized organs were extracted with ethyl acetate, and supernatant fluid was collected and evaporated to dryness. The dry residues were dissolved in methanol for high-performance liquid chromatography analyses.

In vitro ***cytotoxicity.*** The growth-inhibitory activities of Q-PEGL on the CT26 and LL/2 cell lines were evaluated by 3-(4,5-dimethylthiazol-2-yl)-2,5-diphenyltetrazolium bromide assay. The CT26 and LL/2 cells were cultured in DMEM containing 10% fetal bovine serum in a 96-well multiplate. Exponentially growing cells at 2×10^5/mL were exposed to each various doses of Q-PEGL or free quercetin with equivalent dose quercetin for various time intervals. The control culture was treated with PEGL, which diluted along with Q-PEGL dilutions. Then, the 3-(4,5-dimethylthiazol-2-yl)-2,5-diphenyltetrazolium bromide solution was added to these wells at different time point. Cell viability was measured by the absorbance at 570 nm.

To quantitative assessment of apoptosis and analysis of cell cycle specificity, flow cytometric analysis was done to identify sub-G_1 cells/apoptotic cells and to measure the percentage of sub-G_1 cells after propidium iodide staining in hypotonic buffer as described (8, 18). Briefly, cells were suspended in 1 mL hypotonic fluorochrome solution containing 50 μg propidium iodide/mL in 0.1% sodium citrate plus 0.1% Triton X-100 and the cells were analyzed by flow cytometer (ESP Elite, Beckman-Coulter, Miami, FL). Apoptotic cells appeared in the cell cycle distribution as cells with a DNA content of less than that of G_1 cells and were estimated with Listmode software.

In vivo ***antitumor activity.*** In the first experiment, CT26-bearing BABL/c mice and LL/2-bearing C57BL/6N mice were coded and divided into seven groups ($n = 10$ for each group). Treatment was initiated when tumor volume was ~90 mm^3. These mice were given i.v. with PBS, PEGL (100 mg/kg), and Q-PEGL (12.5, 25, 50, 100, and 200 mg/kg), respectively. All these reagents were given every 3 days for 15 days. The mice were sacrificed on day 18 to ascertain the size of tumor lesions, and excised tumors were weighed.

In the second study, the tumor-bearing BABL/c mice inoculated with CT26 cells and C57BL/6N mice with LL/2 cells were coded and divided into four groups ($n = 10$ for each group). These mice were given i.v. with Q-PEGL (50 mg/kg), free quercetin (50 mg/kg), free quercetin (50 mg/kg) plus PEGL (100 mg/kg), and PBS, respectively. All these treatment were given every 3 days for 15 days. Then, these mice were sacrificed on day 18 to ascertain the size of tumor lesions, and excised tumors were weighed as above.

In the third study, tumor-bearing mice inoculated with CT26, H22, and LL/2 cells were classified into three groups ($n = 10$ for each group). In each tumor-bearing mice model, mice were i.v. given with Q-PEGL (50 mg/kg every 3 days for 21 days), DDP (5 mg/kg on days 1, 8, and 15) for positive control groups, and PBS (0.2 mL every 3 days for 21 days) for negative control groups. DDP was dissolved in 0.9% normal solution. Survival time and tumor volumes were observed. Tumor size was determined by caliper measurement of the largest and perpendicular diameters every other day. Tumor volumes were calculated according to the formula: $V = a \times b^2 \times 0.52$, where a is the largest superficial diameter and b is the smallest superficial diameter. The mice were sacrificed when they became moribund. Then, the sacrificed date was recorded to calculate the survival time. To detect the microvessel density, apoptosis, and HSP70 expression, tumors tissues excised were fixed in 10% formalin and frozen in −80°C.

Detection of HSP70 mRNA expression in tumor tissues with quantitative real-time PCR. Quantitative real-time PCR was done to confirm HSP70 expression in tumor tissues. The HSP70-specific primers are as follows: forward primer 5V-CGAGAGCCGGTCGTTCTTC-3V and reverse primer 5V-CAGGTACGCCTCAGCGATCT-3V. The amplified fragment was 202 bp. The probe of HSP70 was 5V-FAM-CGTCCATGGTGCTGACGAAGATGAAG-TAMRA-3V. β-Actin mRNA expression was used to normalize the results.

Total RNA was extracted from tumor tissues (50 mg) by acid-guanidinium thiocyanate-phenol-chloroform (19). The RNA was resuspended in diethyl pyrocarbonate–treated water and quantitated spectrophotometrically for analysis. Reverse transcription reactions were carried out according to Wong et al. (20). Briefly, the percentage efficiency for reverse transcription reactions was estimated to be 69 ± 1.9 (mean ± SE for $n = 7$). The PCR profile was denaturing at 94.8°C for 30 seconds, annealing at 55.8°C for 30 seconds, and extension at 72.8°C for 30 seconds. In each case, the number of cycles was 35. PCR was carried out in a Perkin-Elmer (Cupertino, CA) 2400 Thermal

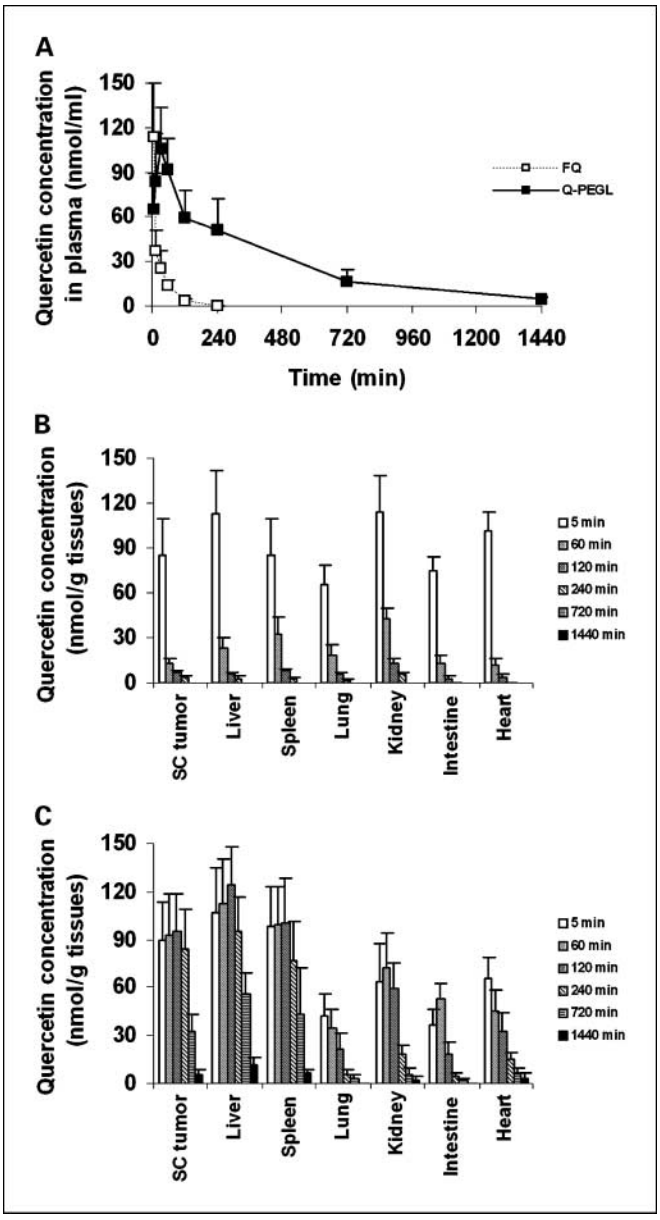

Fig. 1. Biodistribution of Q-PEGL (■) and free quercetin (□) in CT26-bearing BABL/c mice. Mice were i.v. treated by Q-PEGL or free quercetin at a dose of 50 mg/kg based on quercetin and sacrificed on 15 days after the inoculation of tumor cells. The quercetin in plasma, normal organs, and tumor tissues was detected by high-performance liquid chromatography as described in Materials and Methods. *A,* concentration-time curve of quercetin in plasma both Q-PEGL and free quercetin (*FQ*). *B* and *C,* tissue distribution of free quercetin (*B*) and Q-PEGL (*C*) in solid tumor tissues and normal organs at different time point. *Columns,* mean (n = 4 per group at each time point); *bars,* SD.

Cycler. Analysis of PCR product capillary electrophoresis was carried out in a 47-cm silica capillary containing POP-4 polymer (PE Applied Biosystems, Branchburg, NJ). Each sample was run for 24 minutes at 60 kJ voltage with 5 seconds of injection time. We did LIFCE in an ABI PRISM 310 Genetic Analyzer (PE Applied Biosystems).

Detection CD31 by immunohistochemistry and apoptosis by terminal deoxynucleotidyl transferase–mediated dUTP nick end labeling in tumor tissues. The antiangiogenesis effects of liposomal quercetin were determined by CD31 immunostaining. The frozen tissue sections were fixed in acetone, incubated, and stained with an antibody reactive to CD31. The sections were then stained with labeled streptavidin biotin reagents. Vessel density was determined by counting the number of microvessels per high-power field in the sections as described (21). Tumor species embedded by paraffin were prepared as described above. Terminal deoxynucleotidyl transferase–mediated dUTP nick end labeling staining was done following the manufacturer's protocol. Four equal-sized fields in tissue sections were randomly chosen and analyzed. The positive staining was evaluated in each field, yielding the density of apoptotic cells (apoptosis index).

Statistical analysis. Data were assayed by ANOVA and Student's t test. For the survival time of animals, Kaplan-Meier curves were established for each group, and the survivals were compared by the log-rank test. Differences between means or ranks as appropriate were considered significant when yielding a $P < 0.05$. Results are presented as means ± SD. Experiments were done at least in duplicate. The half-lives were calculated using a numerical module of the 3P97 computer program (Chinese Pharmacological Society) for kinetic analysis. The data were fitted into a biexponential equation with a bolus injection as an experimental model.

Results

Pharmacokinetics and tissue distribution of Q-PEGL. After i.v. Q-PEGL, quercetin released from pegylated liposomes quickly conjuncted with glucuronide. Glucosidase was added into plasma sample to break the conjugation and detect free quercetin by high-performance liquid chromatography. Our results show that Q-PEGL prolonged blood circulation times in BALB/c tumor-bearing mice in comparison with free quercetin. The lifetime of Q-PEGL is 2 hours in the plasma, but the lifetime of free quercetin only 5 minutes. The maximum concentration of quercetin in the plasma was 105.6 ± 17.5

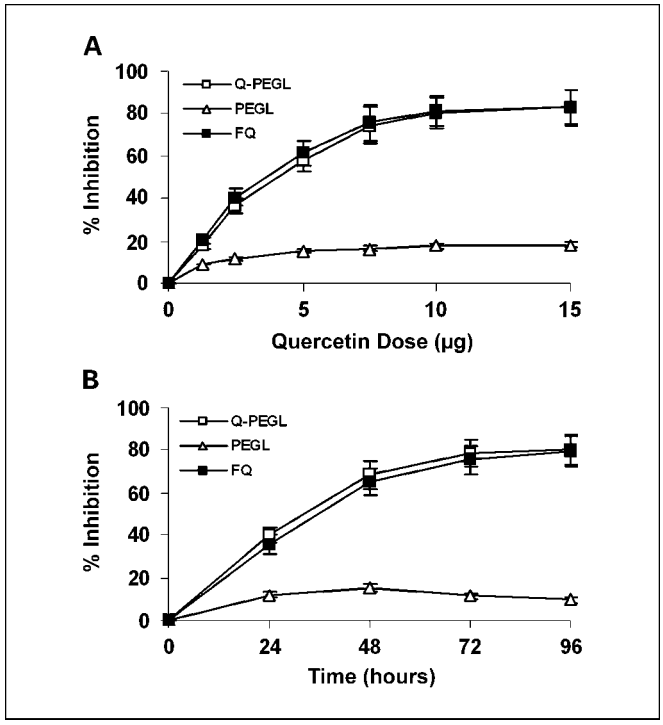

Fig. 2. Dose- and time-dependent inhibition of proliferation of CT26 cells treated with Q-PEGL (■), free quercetin (□), and PEGL (△). *A,* CT26 cells were treated with various doses of Q-PEGL, free quercetin, or PEGL for 36 hours. During the antiproliferative assays, the PEGL concentration in the Q-PEGL was always the same as PEGL. *B,* CT26 cells were treated with Q-PEGL (10 μg/mL based on quercetin), free quercetin (10 μg/mL), and PEGL (30 μg/mL). Cell viability was detected by 3-(4,5-dimethylthiazol-2-yl)-2,5-diphenyltetrazolium bromide assays for various time intervals. Similar results were also found in LL/2 cells.

nmol/mL for the Q-PEGL at time point of 30 minutes and 113.5 ± 23.5 nmol/mL for the free quercetin at time point beginning to detected (Fig. 1A). The levels of quercetin could be still detected at 1,440 minutes for Q-PEGL in plasma.

In the mice treated by free quercetin, quercetin was widely distributed in normal organs and s.c. tumor tissues, and the concentrations of quercetin were relatively high in kidney and liver, moderate in spleen and tumor tissues, and low in lung. These results were consistent to other reports because free quercetin was rapidly cleared up in plasma (Fig. 1A and B). When encapsulated with PEG, quercetin was highly accumulated in liver, tumor tissues, and spleen but low in kidney and lung tissues (Fig. 1C) and had a long retention time in liver, spleen, and tumor tissues. These results show that Q-PEGL could selectively accumulate in s.c. tumor tissues and lengthen retention time at tumor site compared with free quercetin (Fig. 1B and C).

Inhibition of cell proliferation by Q-PEGL treatment. The Q-PEGL treatment resulted in inhibition of cell proliferation *in vitro*, which has similar antiproliferative effect compared with free quercetin. The inhibition effect was dependent on the dose of Q-PEGL and incubation time. For example, when CT26 cells were treated for 36 hours, the percentage inhibition of 1 and 10 μg/mL Q-PEGL was 21% and 71.5%, respectively (Fig. 2A). When CT26 cells were treated by 10 μg/mL Q-PEGL, the percentage inhibition was 42% for 24 hours and 81% for 96 hours (Fig. 2B). The PEGL could also inhibit CT26 cell proliferation but did not show such time- and dose-dependent effect.

By the use of flow cytometry, we could assess the number of sub-G_1 cells (apoptotic cells). Results obtained with flow cytometry strongly show that the Q-PEGL lead to the CT26 death by inducing apoptosis. The quantitative assessment of sub-G_1 cells by flow cytometry was used to estimate the number of apoptotic cells. The apoptosis-inducing effect of Q-PEGL was dose and time dependent, being observed at 1 μg/mL and reaching a maximum at 15 μg/mL when analyzed by flow cytometry. The increased number of apoptotic cells was detected after 12 hours of continuous Q-PEGL treatment, reaching a maximum by 60 hours (Fig. 3).

In vivo *antitumor activity.* In the first test, CT26-bearing BABL/c mice and LL/2-bearing C57BL/6N mice were treated with Q-PEGL at different dose. The mice treated with 12.5 and 25 mg/kg Q-PEGL showed moderate inhibition response to the tumor. The 50 and 100 mg/kg almost have no difference in inhibiting the tumor growth ($P > 0.05$), but the 100 mg/kg group significantly reduced the lung metastases in LL/2-bearing C57BL/6N mice. There was no difference between PBS and PEGL control ($P > 0.05$). The mice treated with 200 mg/kg resulted in death of 3 to 10 after the Q-PEGL administration. Therefore, we selected the dose of 50 mg/kg as effective dose.

In the second study, the free quercetin was found to have antitumor efficiency in inhibiting tumor progress compared with PBS ($P < 0.05$). Free quercetin plus PEGL did not enhance the antitumor efficiency compared with single free quercetin ($P > 0.05$). There was difference between free quercetin plus PEGL and Q-PEGL in inhibiting tumor progress although both with same dose based on quercetin ($P = 0.0014$). The antitumor efficiency of the Q-PEGL groups was better than that of the free quercetin groups.

In the third test, tumor volumes and life span of mice assay showed that the suppression of tumor growth in the Q-PEGL groups was more effective than the PBS control. The Q-PEGL groups resulted in a 40-day survival rate of 40% and decreased the tumor volume versus the PBS control. The inhibition rate of tumor volume treated with Q-PEGL was 45% compared with PBS. The Q-PEGL treatment had resulted in 10-, 11-, and 9-day (DDP 14-, 16-, and 15-day) delay of tumor growth to reach a volume of 900 mm^3 compared with PBS control in CT26, H22, and LL/2 tumor-bearing mice, respectively (Fig. 4A-C). In the CT26, H22, and LL/2 tumor models, control animals that received PBS treatment survived 28.5, 28.5, and 29 days on average, respectively. In contrast, systemic therapy with Q-PEGL significantly resulted in improving the survival time versus PBS ($P < 0.01$, log-rank test; Fig. 4D-F). However, no complete reaction was found in these groups treated with Q-PEGL. Additionally, the appearance of lung metastases in the LL/2

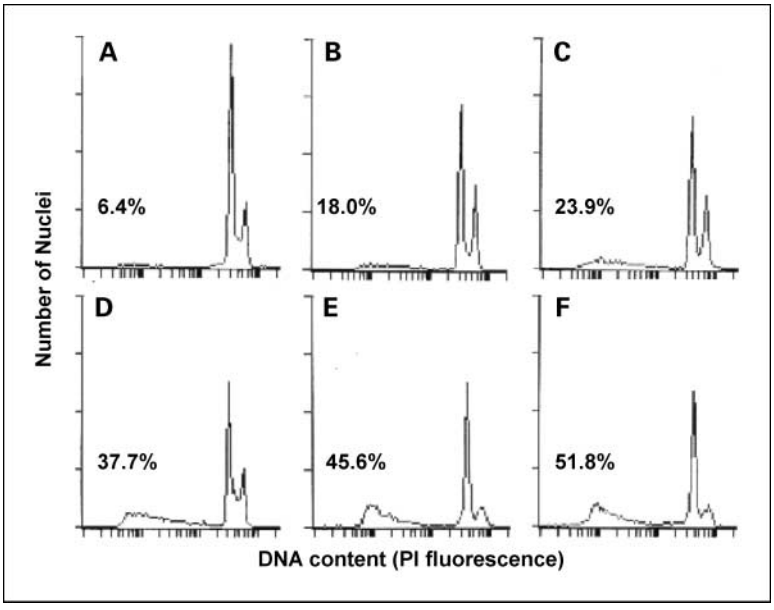

Fig. 3. Representative DNA fluorescence histograms of propidium iodide (*PI*) – stained cells. CT26 cells were untreated (*A*) or treated with 5 μg/mL Q-PEGL for 12 (*B*), 24 (*C*), 36 (*D*), 48 (*E*), and 60 (*F*) hours. The cells in sub-G_1 phase were considered as apoptotic cells. The apoptosis rates in nontreated and Q-PEGL-treated cells were 6.4% (*A*), 18.0% (*B*), 23.9% (*C*), 37.7% (*D*), 45.6% (*E*), and 51.8% (*F*) as assessed by flow cytometry.

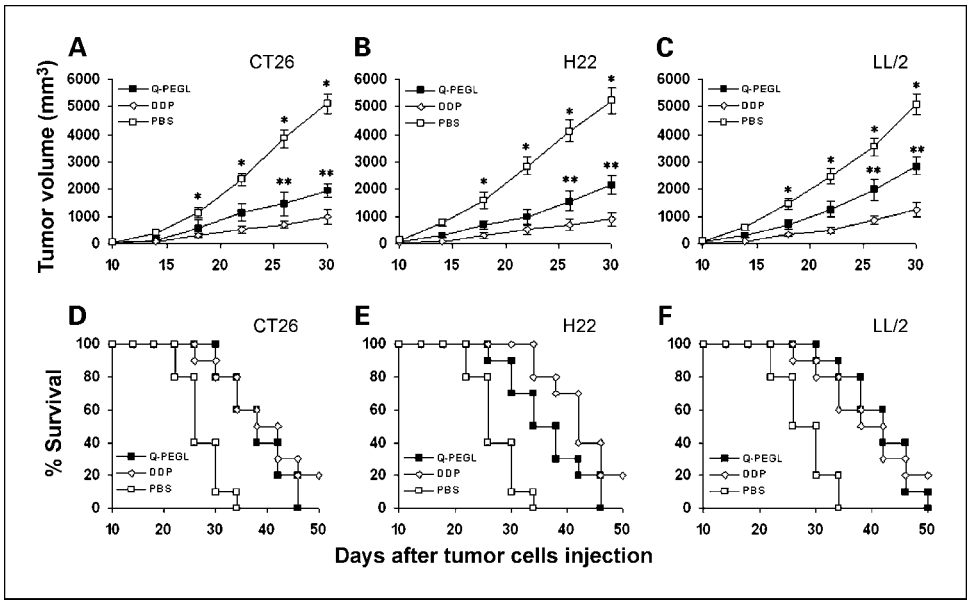

Fig. 4. Tumor suppression and survival advantage in mice. In each tumor-bearing mice model, mice were divided into three groups (n = 10 for each group) and i.v. given with Q-PEGL (■) 50 mg/kg every 3 days for 21 days, DDP (◇) 5 mg/kg on days 1, 8, and 15 after initiation of Q-PEGL treatment, and PBS (□), respectively. *A* to *C,* suppression of tumor growth in Q-PEGL-treated groups, compared with the PBS control, was found in the three tumor models. *Points,* mean; *bars,* SD. *, $P < 0.05$, Q-PEGL versus PBS control; **, $P < 0.05$, Q-PEGL versus DDP control. *D* to *F,* an increase in survival in the Q-PEGL-treated groups, compared with the PBS control ($P < 0.01$, log-rank test), was found in the three tumor models. The survival rate of the mice was 40%, 50%, and 40% on day 40 for mice inoculated with CT26, H22, and LL/2 cells, respectively.

tumor model was significantly delayed by treatment with Q-PEGL in comparison with PBS control.

Q-PEGL inhibited HSP70 expression in tumor tissues. Our studies showed that the antitumor efficacy of Q-PEGL was correlated with HSP70 expression in tumor tissues revealed by quantitative real-time PCR analysis. The relative levels of HSP70 expression were little detected in Q-PEGL group but highly found in the DDP and PBS groups in CT26, LL/2, and H22 tumor-bearing mice model ($P < 0.01$; Fig. 5).

Q-PEGL inhibited angiogenesis and induced apoptosis. Mi-Microvessel density was quantified to measure angiogenesis by immunolabeling of CD31 in frozen tumor tissue sections. The most highly vascularized area of each tumor was identified on low power, and five high-power fields were counted in this area of greatest vessel density. The Q-PEGL apparently reduced the number of vessels compared with PBS or DDP alone ($P < 0.05$). There was no difference between DDP and PBS in microvessel density ($P < 0.05$; Fig. 6A-C).

The tumor tissues were subjected to terminal deoxynucleotidyl transferase–mediated dUTP nick end labeling assays for respective determination of apoptotic index. Both the Q-PEGL group and the DDP group have a high apoptosis rate of tumor cells compared with the PBS control ($P < 0.05$). There was no difference between DDP and Q-PEGL in apoptotic index ($P > 0.05$; Fig. 6D-F).

Discussion

High and selective accumulation of chemotherapeutic drugs at the tumor site is essential for the success of drug treatment *in vivo*. Previous studies have reported that quercetin in rats were widely distributed in tissues, with the highest concentrations in lungs and the lowest in brain, white fat, and spleen (22). Our studies showed that Q-PEGL can selectively accumulate in tumor site in comparison with free quercetin. Furthermore, Q-PEGL can significantly improve the water insolubility of quercetin, prolong the circulation times in the blood, and enhance antitumor efficacy.

Previous studies *in vitro* and *in vivo* identified that anticancer agents encapsulated by pegylated liposome can significantly prolong the plasma residence time of drugs that would otherwise be rapidly distributed or cleared (14, 23–26). Altered plasma pharmacokinetics is one mechanism by which liposomal drugs may show substantial changes in tissue distribution, efficacy, and toxicity from their free drugs. Increasing therapeutic efficacy was found in these liposomal drugs. These benefits derive from the altered pharmacokinetics and biodistribution afforded by the liposomal carrier. This may be especially important for water insolubility natural plant, such as quercetin. Increasing lifetime of Q-PEGL in the plasma compared with that of free quercetin was seen in our studies. Biodistribution studies showed that Q-PEGL was high concentration accumulated in tumor tissues. Thus, the increase in antitumor efficacy seen in the present experiments may be due to prolong exposure as determined by the increase in plasma half-time and to accumulation of the drug at the tumor site.

Defects in the capillary endothelium of tumor vasculature are typically in the size range of 400 to 600 nm; therefore, liposomes having diameters smaller than 400 nm can

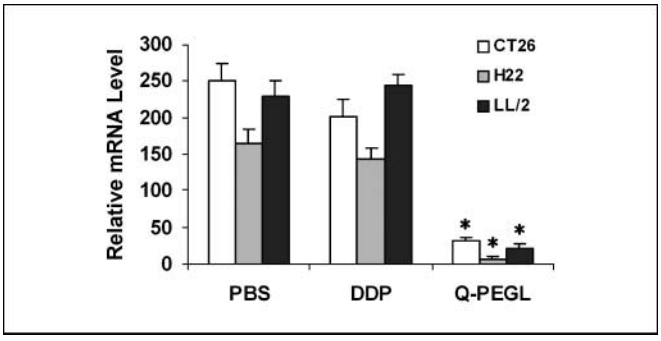

Fig. 5. Relative level of HSP70 mRNA expression in tumor tissues detected by quantitative real-time PCR analysis. In each tumor model, mice were divided into three groups (n = 10 for each group) and treated with Q-PEGL, DDP, and PBS, respectively. Tumor tissues (50 mg) were collected for quantitative real-time PCR analysis at autopsy as described in Materials and Methods. *Columns,* mean; *bars,* SD. *, $P < 0.05$ (Q-PEGL versus PBS or DDP alone control).

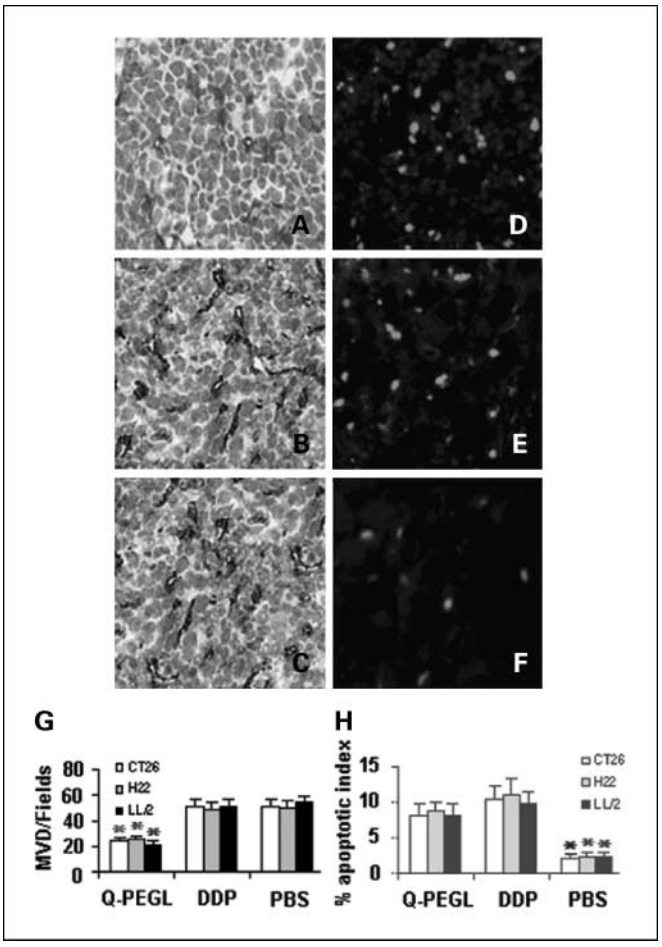

Fig. 6. Inhibition of angiogenesis assayed by immunohistochemistry with CD31 and terminal deoxynucleotidyl transferase – mediated dUTP nick end labeling staining of tumor tissues. The tumor-bearing mice were divided into three groups in each tumor model ($n = 10$ for each group). These mice were given i.v. with Q-PEGL (*A* and *D*), DDP (*B* and *E*), and PBS (*C* and *F*), respectively. Microvessel and apoptosis counting were done at ×200. Representative sections from CT26 tumor tissue. *A* to *C,* tumor angiogenesis was assessed by immunohistochemical staining with anti-CD31 antibody (*brown*) on paraffin-embedded sections of tumors dissected after completion of treatment. Q-PEGL-treated revealed angiostatic effect in tumor tissues compared with DDP (*B*) and PBS (*C*). *, $P < 0.05$, Q-PEGL versus PBS or DDP alone control. *D* to *F,* terminal deoxynucleotidyl transferase – mediated dUTP nick end labeling staining of tumor tissues. Q-PEGL (*D*) or DDP (*E*) alone showed an effective induction of apoptosis compared with PBS control. *Columns,* mean; *bars,* SD. *, $P < 0.05$, Q-PEGL or DDP alone versus PBS control.

efficiently extravasate and accumulate within the tumor interstitial space (15). Otherwise, tumors have impaired lymphatic drainage (27), which makes extravasated liposomal drug have a long retention time in tumor tissues (13). An earlier study showed that large multilamellar vesicles have limited value as drug carriers because of their rapid clearance from the circulation (28). In addition, liposomes of small unilamellar vesicles are easily prone to endocytosis and are taken up by a large number of solid tumors due to the enhanced permeability and retention effect (29, 30). In present studies, the diameter of Q-PEGL was examined no more than 150 nm, which was favorable to increase quercetin concentration in tumor tissues.

Caltagirone et al. (31) have observed that quercetin given *in vivo* reduce the melanoma growth and metastasis in mice. In phase I and II clinical trials, Ferry et al. (32) found that i.v. quercetin could inhibit tumor progress in hepatocellular carcinoma and ovarian cancer, but the vehicle, DMSO, is unsuitable for further clinical development of quercetin. In our studies, the free quercetin could inhibit mouse colon carcinoma and Lewis lung cancer growth *in vivo*, but the antitumor efficiency of free quercetin was significantly less than that of Q-PEGL with equivalent dose quercetin.

It is known that members of the HSP70 families are often associated with cell cycle – related proteins, including p53, Cdk4, c-myc, pRb, and p27 (33 – 34). Compared with the corresponding normal tissues, increased amounts of cytoplasmic HSP70 have been found in lung, colorectum, and liver carcinomas (35 – 37). Recently, HSP70 overexpression has been identified as a marker of poor prognosis in many malignant tumors (38). Current results confirmed that HSP70 expression in tumor tissues was obviously down-modulated in mice treated by quercetin and apoptosis was increased. Such results were not found in DDP-treated mice group. There may be different antitumor mechanism between quercetin and DDP in inducing tumor cell apoptosis.

Although the present results show a significant suppression of tumor growth *in vivo* by Q-PEGL, it should be pointed out that the treatment of mice with Q-PEGL did not result in the complete eradication of the tumor cells with the dose and schedules used in this study. The tumor rapidly grew after cease the usage of Q-PEGL. Although Q-PEGL significantly prolonged the mean survival time of the mice, all of the survived animals died within 50 days in these models because of the big volume of tumor tissue and metastasis. This may be partly attributed to the fact that Q-PEGL was given every 3 days partly to a limited penetration of these long-circulating liposomes into the interior of established solid tumors *in vivo* (39). Clearly, additional development of these liposomal formations should be pursued to rectify these deficiencies. Detailed pharmacokinetic studies are in progress to improve antitumor efficacy and further antitumor mechanism of quercetin *in vivo* is being explored in our laboratory.

In conclusion, this study showed that the Q-PEGL could effectively accumulate in tumor tissues, lengthen the circulation time of quercetin *in vivo*, effectively inhibit multiple kinds of tumor growth, and prolong the survival time of tumor-bearing mice. Solid tumors belong to the most aggressive human cancers with short survival times. It is encouraged that the Q-PEGL could archive such good efficacy in the several solid tumor models. It is also important to note that Q-PEGL was unable to inhibit tumor growth fully. It is necessary to optimize liposomal formations and therapeutic schema to obtain better therapeutic efficacy.

References

1. Swain T. The flavonoids. London: Chapman & Hall; 1975.
2. Formica JV, Regelson W. Review of the biology of quercetin and related biofavonoids. Food Chem Toxicol 1995;33:1061 – 80.
3. Castillo MH, Perkins E, Campbell JH, et al. The effects of the bioflavonoid quercetin on squamous cell carcinoma of head and neck origin. Am J Surg 1989;158: 351 – 35.
4. Scambia G, Ranelletti FO, Benedetti PP, et al. Quercetin inhibits the growth of a multidrug-resistant estrogen-receptor-negative MCF-7 human breast-cancer cell line expressing type II estrogen-binding sites. Cancer Chemother Pharmacol 1991; 28:255 – 8.
5. Ranelletti FO, Ricci R, Larocca LM, et al. Growth-inhibitory effect of quercetin and presence of type-II estrogen-binding sites in human colon-cancer cell

lines and primary colorectal tumors. Int J Cancer 1992; 50:486–92.

6. Elattar TM, Virji AS. The inhibitory effect of curcumin, genistein, quercetin and cisplatin on the growth of oral cancer cells *in vitro*. Anticancer Res 2000;20: 1733–8.

7. Nair HK, Rao KV, Aalinkeel R, et al. Inhibition of prostate cancer cell colony formation by the flavonoid quercetin correlates with modulation of specific regulatory genes. Clin Diagn Lab Immunol 2004;11:63–9.

8. Wei YQ, Zhao X, Kariya Y, et al. Induction of apoptosis by quercetin: involvement of heat shock protein. Cancer Res 1994;54:4952–7.

9. Muther RS, Bennett WM. Ejects of dimethyl sulfoxide on renal function in man. JAMA 1980;244:2081–3.

10. Marshall LF, Camp PE, Bowers SA. Dimethyl sulfoxide for the treatment of intracranial hypertension: a preliminary trial. Neurosurgery 1984;14:659–63.

11. Rijtema M, Mosig D, Drukker A, Guignard JP. The effects of dimethyl sulfoxide on renal function of the newborn rabbit. Biol Neonate 1999;76:355–61.

12. Mulholland PJ, Ferry DR, Anderson D, et al. Preclinical and clinical study of QC12, a water-soluble, pro-drug of quercetin. Ann Oncol 2001;12:245–8.

13. Allen TM, Cullis PR. Drug delivery systems: entering the mainstream. Science 2004;19:1818–22.

14. Batist G, Ramakrishnan G, Rao CS, et al. Reduced cardiotoxicity and preserved antitumor efficacy of liposome-encapsulated doxorubicin and cyclophosphamide compared with conventional doxorubicin and cyclophosphamide in a randomized, multicenter trial of metastatic breast cancer. J Clin Oncol 2001; 19:1444–54.

15. Yuan F, Dellian M, Fukumura D, et al. Vascular permeability in a human tumor xenograft: molecular size dependence and cutoff size. Cancer Res 1995;55: 3752–6.

16. Harris JM, Chess RB. Effect of pegylation on pharmaceuticals. Nat Rev Drug Discov 2003;2:214–21.

17. Lu Y, Wei YQ, Tian L, et al. Immunogene therapy of tumors with vaccine based on xenogeneic epidermal growth factor receptor. J Immunol 2003;170:3162–70.

18. Peng F, Wei YQ, Tian L, et al. Induction of apoptosis by norcantharidin in human colorectal carcinoma cell lines: involvement of the CD95 receptor/ligand. J Cancer Res Clin Oncol 2002;128:223–30.

19. Chomczynski P, Sacchi N. Single-step method of RNA isolation by acid guanidinium thiocyanate-phenol-chloroform extraction. Anal Biochem 1987; 162:156–9.

20. Wong H, Anderson WD, Cheng T, Riabowol KT. Monitoring mRNA expression by polymerase chain reaction: the "primerdropping" method. Anal Biochem 1994;223:251–8.

21. Blezinger P, Wang J, Gondo M, et al. Systemic inhibition of tumor growth and tumor metastases by intramuscular administration of the endostatin gene. Nat Biotechnol 1999;17:343–8.

22. de Boer VC, Dihal AA, van der Woude H, et al. Tissue distribution of quercetin in rats and pigs. J Nutr 2005;135:1718–25.

23. Lee CM, Tanaka T, Murai T, et al. Novel chondroitin sulfate-binding cationic liposomes loaded with cisplatin efficiently suppress the local growth and liver metastasis of tumor cells *in vivo*. Cancer Res 2002; 62:4282–8.

24. Tardi P, Choice E, Masin D, et al. Liposomal encapsulation of topotecan enhances anticancer efficacy in murine and human xenograft models. Cancer Res 2000;60:3389–93.

25. Emerson DL, Bendele R, Brown E, et al. Antitumor efficacy, pharmacokinetics, and biodistribution of NX 211: a low-clearance liposomal formulation of lurtotecan. Clin Cancer Res 2000;6:1903–12.

26. Boman NL, Bally MB, Cullis PR, Mayer LD, Webb MS. Encapsulation of vincristine in liposomes reduces toxicity and improves antitumor efficacy. J Liposome Res 1995;5:523–41.

27. Jain RK. Transport of molecules across tumor vasculature. Cancer Metastasis Rev 1987;6:559–93.

28. Torchilin VP. Recent advances with liposomes as pharmaceutical carriers. Nat Rev Drug Discov 2005; 4:145–60.

29. Mayer LD, Tai LC, Ko DS, et al. Influence of vesicle size, lipid composition, and drug-to-lipid ratio on the biological activity of liposomal doxorubicin in mice. Cancer Res 1989;49:5922–30.

30. Forssen EA, Coulter DM, Proffitt RT. Selective *in vivo* localization of daunorubicin small unilamellar vesicles in solid tumors. Cancer Res 1992;52: 3255–61.

31. Caltagirone S, Rossi C, Poggi A, et al. Flavonoids apigenin and quercetin inhibit melanoma growth and metastatic potential. Int J Cancer 2000;87: 595–600.

32. Ferry DR, Smith A, Malkhandi J, et al. Phase I clinical trial of the flavonoid quercetin: pharmacokinetics and evidence for *in vivo* tyrosine kinase inhibition. Clin Cancer Res 1996;2:659–68.

33. Jolly C, Morimoto RI. Role of the heat shock response and molecular chaperones in oncogenesis and cell death. J Natl Cancer Inst 2000;92:1564–72.

34. Zylicz M, King FW, Wawrzynow A. Hsp70 interactions with the p53 tumour suppressor protein. EMBO J 2001;20:4634–8.

35. Bonay M, Soler P, Riquet M, et al. Expression of heat shock proteins in human lung and lung cancers. Am J Respir Cell Mol Biol 1994;10:453–61.

36. Luk JM, Lam CT, Siu AF, et al. Proteomic profiling of hepatocellular carcinoma in Chinese cohort reveals heat-shock proteins (Hsp27, Hsp70, GRP78) up-regulation and their associated prognostic values. Proteomics 2006;6:1049–57.

37. Banerjea A, Feakins RM, Nickols CD, et al. Immunogenic hsp-70 is overexpressed in colorectal cancers with high-degree microsatellite instability. Dis Colon Rectum 2005;48:2322–8.

38. Ciocca DR, Caldlerwood SK. Heat shock proteins in cancer: diagnostic, prognostic, predictive, and treatment implications. Cell Stress Chaperones 2005;10: 86–103.

39. Bandak S, Goren D, Horowitz A, Tzemach D, Gabizon A. Pharmacological studies of cisplatin encapsulated in long-circulating liposomes in mouse tumor models. Anticancer Drugs 1999;10: 911–20.